Emergency Load Shedding Strategy with Warning and Delay Time Based on Energy Storage

Pengfei Yu, Xiaofu Xiong, Xiangzhen He, Jizhong Zhu, Jun Liang, and Dongliang Nan

***Abstract*—Considering the escalating usage of renewable energy and rising frequency of extreme meteorological events, the risk of emergency load shedding (ELS) in power grids due to faults is increasing. The existing ELS strategies fail to provide users with advance warnings and blackout preparation time. To address this issue, an innovative strategy called warning and delayed load shedding is proposed in this study. In this approach, when it becomes necessary to shed load for emergency control, users are immediately notified with a power outage warning. Subsequently, energy storage and other regulatory resources are employed to substitute for load shedding, thus postponing the execution of the load shedding command. This delay equips users with the ability and time to respond and prepare. To implement this strategy, the operational principles supported by energy storage and backup power are further discussed. Five performance indexes are utilized to evaluate the delayed load shedding capability. Moreover, the delayed load shedding switch function and energy storage power balance equation are constructed to determine the relationship between energy storage, backup power sources, and load shedding time. Subsequently, two optimized load shedding models supported by energy storage are established, i.e., maximum and flexible delayed models. For comparison, improvements are made to the conventional load shedding model without delay by incorporating energy storage. An IEEE 30-node network with energy storage is used to test the three load shedding models. Accordingly, the evaluation indexes are calculated and compared. The results of the performance indexes and comparative analysis validate the effectiveness of the proposed methods, indicating that by using energy storage, users can be notified with advance power outage warnings and preparation time.**

***Index Terms*—Delayed load shedding, load shedding evaluation index, load shedding warning, emergency load shedding, unscheduled outage.**

Received: January 5, 2024
Accepted: April 1, 2024
Published Online: July 1, 2025

Pengfei Yu is with the School of Electrical Engineering, Chongqing University, Chongqing 400044, China; and also with Chongqing Hui Zhi Energy Co., Ltd., Chongqing 400042, China (e-mail: ypf883@hotmail.com).

Xiaofu Xiong (corresponding author) and Xiangzhen He are with the School of Electrical Engineering, Chongqing University, Chongqing 400044, China (e-mail: cquxxf@vip.sina.com; hxzee@foxmail.com).

Jizhong Zhu is with the School of Electrical Power Engineering, South China University of Technology, Guangdong 510641, China (e-mail: zhujz@scut.edu.cn).

Jun Liang is with the School of Engineering, Cardiff University, Cardiff CF24 3AA, UK (e-mail: LiangJ1@cf.ac.uk).

Dongliang Nan is with the Electric Power Research Institute of State Grid Xinjiang Electirc Power Co., Ltd., Urumqi 830063, China (e-mail: ndl__hhu@126.com).

DOI: 10.23919/PCMP.2024.000090

I. Introduction

Ensuring the reliability and safety of power supply for electricity users has always been a priority of the power system [1], [2]. However, given the challenges posed by equipment maintenance, equipment faults, external disasters, etc., power outages are inevitable. Compared with planned power outage events, unplanned power outages have a greater impact on users. This is mainly because emergency load shedding (ELS) in power grids can lead to insufficient preparation for a large number of users, resulting in load losses and safety risks such as the shutdown of public facilities [3], [4].

In recent years, several challenges such as the increased instability in power grids caused by the rising penetration of renewable energy, frequent grid faults due to adverse weather conditions, and severe power imbalance between the sending and receiving power systems resulting from faults in ultra-high-voltage, large-capacity, and long-distance transmission systems, have contributed to the heightened likelihood of unplanned power outages for electricity users [5]. To mitigate the severe impact of unplanned power outages on users, it is necessary to explore enhanced strategies to tackle ELS. This involves implementing advance warnings before load shedding, and allowing a delay period before initiating shedding to provide users with sufficient time to prepare for the outage.

At present, the research on ELS is primarily conducted considering three perspectives, i.e., the grid, distribution and users.

A. ELS Defense Strategies on Grid Side

In large-scale AC-DC interconnected power grids, a substantial cutoff of high-power DC injection may cause issues such as severe power deficiency and component heating in the receiving AC grid due to adjustments in load flow. Therefore, there is a need for ELS at a few nodes to maintain power balance in the receiving AC grid. Hence, a stratified optimization strategy is proposed for load shedding in the receiving-end power grid [6]. For voltage levels of 500 kV and above, the objective involves minimizing the total load shedding, whereas for voltage levels below 500 kV, a load shedding strategy is employed based on a fuzzy comprehensive evaluation that considers more load

characteristics, including load importance, load carrying capacity, and load flexibility, to reduce the impact of load shedding. Although this method prioritizes the speed of load shedding and considers load characteristics, it does not alter the abrupt nature of load shedding.

In DC interconnected power systems, when urgent load control is required owing to faults at the sending or receiving end, a combined approach of ELS and power regulation in DC transmission lines can be employed. This achieves inter-area coordinated control, thus minimizing the amount of load shedding to the greatest extent [7]. However, this method is only applicable to DC interconnected power systems and their specific operational modes.

In DC systems, to address the risk of voltage instability and subsequent load shedding resulting from grid faults, an intelligent two-stage pre-decision method for ELS is proposed in [8]. The first stage involves determining the load shedding points, whereas the second stage focuses on deciding the amount of load shedding. The total amount required for system recovery is directly estimated from simulation data and then allocated according to the priority levels of loads. However, given the stochastic nature of grid risks, it remains challenging to inform users to take preventive measures based on the estimated load shedding amount.

In AC power systems, considering the influence of power variations during the electromechanical transient process following fault clearance, a method combining electromechanical transient simulation and heuristic artificial intelligence is used in [9]. This approach enhances the ELS optimization algorithm in terms of generation and update of the particle swarm, thereby improving the precision of load shedding.

To address the insufficient consideration of load characteristics in AC for ELS, a strategy considering user costs is proposed in [10]. It establishes a multi-objective optimization model for non-cooperative games, with the objective function of minimizing the payment function for each user.

To address the ignorance of distributed energy sources in current load shedding practices, a feeder-level net load decomposition method is employed in [11] that can separate distributed photovoltaic (PV) power and identify load components. It addresses the challenge of accurate power estimation of a large number of PV energy sources.

B. ELS Defense Strategies on Distribution Side

On the distribution side, to cope with large-scale grid power outages, constructing active distribution networks [12], [13] and microgrids [14]–[16], isolated operation [17] and black start [18], [19] after a major power grid outage can be realized. However, owing to the capacity limitations of distributed energy sources and energy storage, it is difficult to provide energy backup for all loads. To ensure power supply to critical loads and support black start, several studies have been conducted on the configuration of mobile power generation devices [20], [21]. These efforts have enhanced the support capabilities of distribution networks during power outages.

Battery energy storage systems can achieve rapid response, thus swiftly providing power and enabling quick transition to backup power in the event of grid faults or emergencies [23]–[25]. Unlike stationary energy storage units, a mobile energy storage system (MESS) can move between different buses via a truck to provide different local services within the distribution feeder. Among these, a key application scenario for MESS is supplying emergency power to critical loads that have been disconnected. However, the moving time of MESS plays a crucial role in influencing the effectiveness of emergency support. Therefore, an intelligent assisted assessment method for distribution grid has been devised [26].

C. ELS Defense Strategies on User Side

On the user side, to manage the impact of sudden power outages, it is mandatory for critical users to be equipped with backup power sources including standby generators, static energy storage devices such as uninterrupted power supply (UPS), dynamic energy storage devices (such as flywheel energy storage), and mobile power generation equipment [27]. When there is a sudden interruption in the power supply, the startup speed and switching time of the backup power source become significantly different [28], which can influence the safety of users.

Critical infrastructures such as medical facilities, data centers, and communication equipment require backup power sources with an instantaneous switchover, such as the widely utilized UPS [29]. For large-scale industrial sectors like petrochemical and steel production, where multiple production lines are in operation, an interruption in power supply over a few frequency cycles can lead to disruptions in the production process and even cause safety accidents [30]. Although high-capacity UPS systems are available, they are costly and pose challenges in maintenance, failing to meet the seamless power supply demands of these industries [31]. Emergency power supply (EPS), functioning as a backup power source, possesses significant power capacity. However, it typically engages only in the event of grid power failure, with a relatively extended transition period, usually ranging from 0.25 s to 5 s [32], [33]. Gas/diesel generator sets are commonly selected as local energy units for EPS in critical infrastructure owing to their sustained and robust power supply capabilities. However, the long startup time from standby mode makes the seamless task and rapid power restoration of critical infrastructure difficult [34].

From the aforementioned studies it can be concluded that the existing ELS strategies have not considered the "suddenness" of load shedding. Moreover, users without backup power can only passively endure the consequences of emergency power outage, whereas even users with backup power sources may still experience load interruptions due to reserve power switchover, making it challenging to completely eliminate the impact on users.

To manage the impact of sudden power outages on users, a method of mitigating the effects through the implementation of advanced warning and delayed load

shedding (WDLS) is proposed in this study. The challenge in adopting WDLS lies in meeting both the grid's demand for load reduction and the users' requirement for delayed power outage during emergency control, thereby providing a rational control model for implementing new emergency control strategies.

The key contributions of this study are stated below.

1) A novel WDLS method based on energy storage is proposed for power ELS. Compared to previous load shedding strategies that do not consider warning and delay, the proposed WDLS strategy offers users a preparation period for power outage, which is advantageous in reducing the impact of power outage on users.

2) A group of indexes are introduced to measure the performance of ELS, providing criteria for future load shedding enhancement.

3) Three optimized load-shedding models are constructed for comparation. The important roles of energy storage for WDLS are proved through case studies. Unlike previous approaches, an optimized control model is introduced for adjusting delay time in load shedding. This enhancement enables the implementation of flexible load shedding strategies tailored to various load backup power types.

The remainder of this paper is organized as follows. Section II presents the new principle of ELS with warning and delay time, while Section III discusses the construction of performance indexes for WDLS and CELS. Section IV gives the optimization model of WDLS based on energy storage. In Section V, the simulations of multi-mode emergency load-shedding control are presented, and Section VI presents the main conclusions of the paper.

II. New Principle of ELS with Warning and Delay Time

A. Operation Process of ELS

When there is an urgent need for load shedding in a power system, the operation is implemented using a hierarchical control approach. A typical provincial power grid system is described in [35]. Figure 1 presents a schematic illustrating the construction of a load control system. This system comprises a master control station, several load control substations, numerous user-side control terminals, and communication equipment.

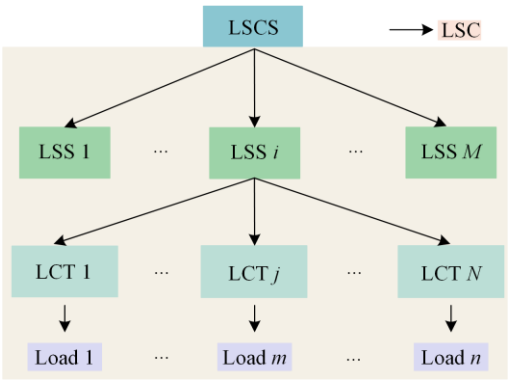

Fig. 1. Traditional load control system.

The load-shedding center station (LSCS) is typically located at critical 500 kV substations, receive load shedding commands (LSC) from the power system safety control center, and load information from load shedding substations (LSS). The LSS allocate the load amount that needs to be switched off based on the priority level, and subsequently, send load-shedding commands to the load control terminal (LCT). Thus, traditional load shedding methods involve the direct disconnection of loads under specific conditions without providing any prior warning before the actions.

B. Improved Operation Process of ELS with Warning and Delay Time

To address the aforementioned issues, a load shedding warning (LSW) signal is introduced before the initiation of LSC in this study, which allows users emergency response times. The proposed improved control system is shown in Fig. 2, while the flowchart for WDLS is depicted in Fig. 3.

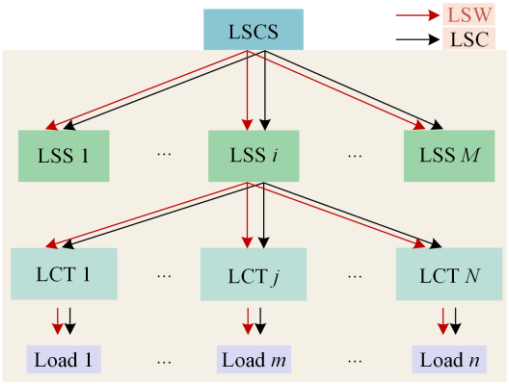

Fig. 2. Improved load control system.

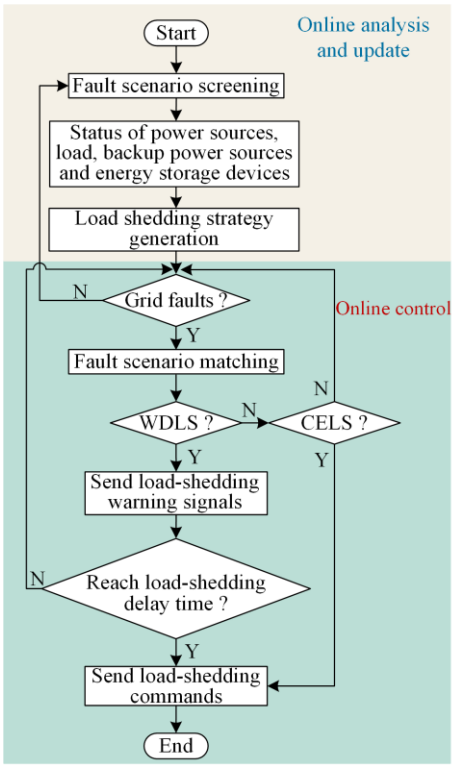

Fig. 3. Flowchart for WDLS and CELS.

As shown in Fig. 3, in this study, ELS is classified into two types: WDLS and conventional emergency load shedding (CELS). Fault scenario analysis is conducted initially to identify scenarios requiring load shedding and determine the optimal load shedding strategy. Subsequently, the pre-decision control table is dynamically updated, including corresponding operating modes and parameters for each power source, network, and load scale. During the "online matching" phase, the pre-decision table is queried in the event of a fault to determine the control mode formulated for the current fault scenario, and WDLS control operations are executed accordingly.

Figure 4 illustrates the differences in time-power characteristics between immediate ELS and WDLS after a fault.

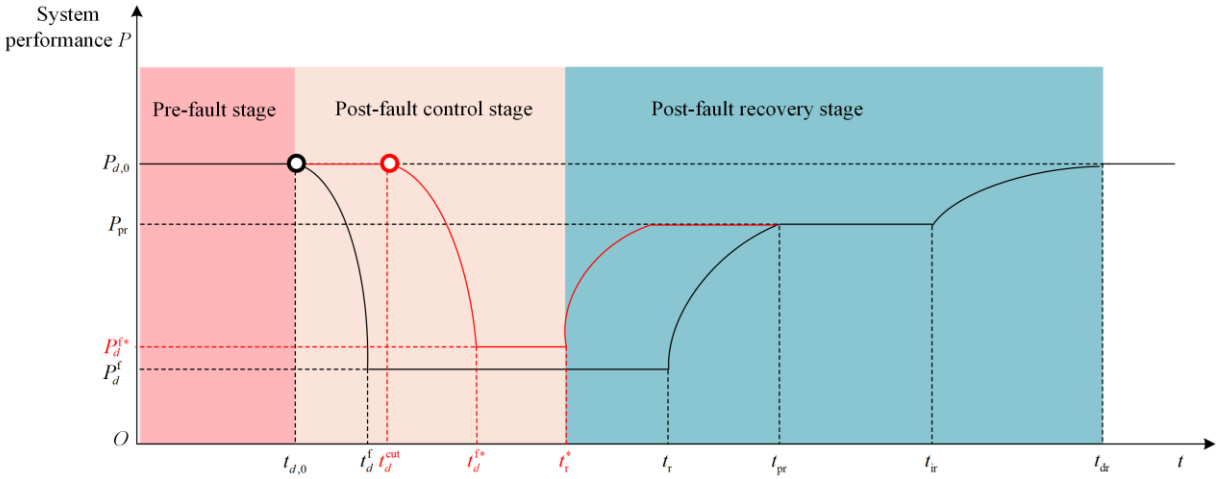

Fig. 4. Time-power curves of different load shedding models.

As seen, the power grid initiates emergency power control to reduce loads after faults, represented by the black line. Thus, the load power decreases from $P_{d,0}$ at time $t_{d,0}$ to P_d^{f} at time t_d^{f}, and the loss of load power P_d^{loss} can be characterized as follows:

$$P_d^{\mathrm{loss}} = P_{d,0} - P_d^{\mathrm{f}} \tag{1}$$

Let $t_{d,0}$ and t_d^{cut} be the start points of the fault and load shedding, respectively, then the delay time of load shedding is:

$$t_d^{\mathrm{dt}} = t_d^{\mathrm{cut}} - t_{d,0} \tag{2}$$

The delay time is from the moment of load-shedding demand to the time the load is switched off.

When load shedding begins immediately after a fault (black line in Fig. 4), $t_d^{\mathrm{cut}} = t_{d,0}$, and $t_d^{\mathrm{dt}} = 0$. When load shedding is not initiated immediately after a fault (red line in the graph), $t_d^{\mathrm{cut}} \neq t_{d,0}$, and $t_d^{\mathrm{dt}} \geqslant 0$.

Typically, after a fault occurrence, the system protection evaluates the fault mode to determine if load shedding is necessary. This study proposes that when load shedding is necessary, advance power outage warnings should be first issued to the users scheduled for load shedding.

The loss of load power for WDLS can be given by:

$$P_d^{\mathrm{loss*}} = P_{d,0} - P_d^{\mathrm{f*}} \tag{3}$$

The differences between WDLS and CELS are illustrated in Fig. 5. In conventional methods, load shedding is initiated before the implementation of emergency response measures, whereas the approach presented in this paper involves initially issuing a blackout warning, which provides users the opportunity to activate emergency measures in advance, and then followed by the load shedding process.

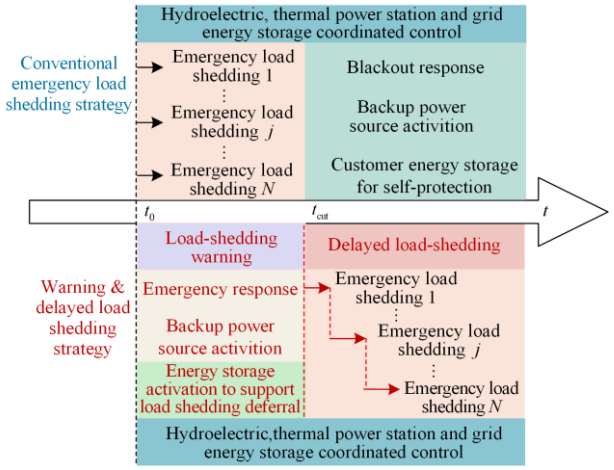

Fig. 5. Differences between CELS and WDLS.

When using delayed load shedding, sudden power outages can be changed to planned outages with advance warnings, thus improving user safety. However, the load shedding power may vary, either exceeding or falling below the levels observed in non-warning load shedding modes.

To achieve WDLS and maintain system power balance, during period t_d^{dt}, it is necessary to rely on backup power sources such as energy storage to rapidly supplement power equivalent to the needs of power balance. Figure 6 shows a power system that includes hydroelectric plants, thermal power plants, and battery energy storages.

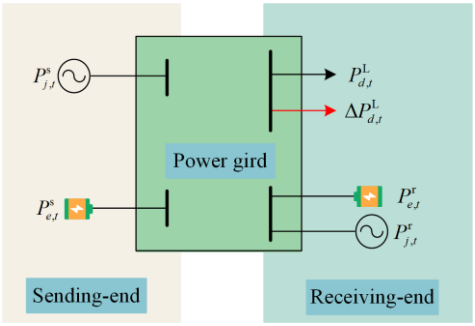

Fig. 6. Power system model with load-shedding.

At moment t, $P_{j,t}^{\mathrm{s}}$ denotes the output of all generating units at the sending end; $P_{e,t}^{\mathrm{s}}$ is the output of all storage plants at the sending end; $P_{j,t}^{\mathrm{r}}$ is the total reserve generating unit output at the receiving end; $P_{e,t}^{\mathrm{r}}$ is the output of all energy storage plants at the receiving end; $P_{d,t}^{\mathrm{L}}$ is the load of all nodes; and $\Delta P_{d,t}^{\mathrm{L}}$ is the amount of cut-load at all nodes.

Before a fault, the power balance should be maintained by the system at all times:

$$P_{j,t}^{\mathrm{s}}+P_{j,t}^{\mathrm{r}}+P_{e,t}^{\mathrm{s}}+P_{e,t}^{\mathrm{r}}=P_{d,t}^{\mathrm{L}} \tag{4}$$

$$P_{j,t}^{\mathrm{s}}+P_{j,t}^{\mathrm{r}}=\sum_{j=1}^{J}P_{j,t} \tag{5}$$

$$P_{e,t}^{\mathrm{s}}+P_{e,t}^{\mathrm{r}}=\sum_{e=1}^{E}P_{e,t} \tag{6}$$

After a fault, considering the switching function $P_{j,t}$ during the load shedding process, the following equation can be obtained:

$$\sum_{j=1}^{J}P_{j,t}+\sum_{j=1}^{J}\Delta P_{j,t}+\sum_{e=1}^{E}P_{e,t}+\sum_{e=1}^{E}\Delta P_{e,t}=\sum_{d=1}^{D}(P_{d,t}+u_{d,t}\Delta P_{d,t}) \tag{7}$$

where $P_{j,t}$ is the output of conventional resource unit j; $P_{e,t}$ is the output of energy storage e; $P_{d,t}$ is the load of node d; $u_{d,t}$ is a state variable with a value of 1 or 0 at time t; $\Delta P_{d,t}$ is the cut-load power of node d; J, E and D correspond to the total numbers of conventional units, storage units and load nodes, respectively; $\Delta P_{j,t}$ and $\Delta P_{e,t}$ are the adjustment quantities for generating units and energy storage, respectively.

If there is a disturbance by a fault that leads to a change in the power network, power source, or power load at time t, the power fluctuation can be expressed as:

$$\sum_{d=1}^{D}u_{d,t}\Delta P_{d,t}=\sum_{j=1}^{J}\Delta P_{j,t}+\sum_{e=1}^{E}\Delta P_{e,t} \tag{8}$$

Equation (8) illustrates that the cutting load power and time depend on controlling the power output of conventional power sources and energy storage.

The amount of energy storage required for regulation is:

$$\Delta P_{E}=\sum_{e=1}^{E}\Delta P_{e,t}=\sum_{d=1}^{D}\Delta P_{d,t}-\sum_{j=1}^{J}\Delta P_{j,t} \tag{9}$$

Equation (9) indicates that if there is sufficient energy storage, the imbalance caused by faults or security constraints between power sources and loads can be compensated.

Because the capacity of energy storage is limited, loads or power resources will be switched off when the energy storage power is exhausted.

Considering that at node d, a portion of the load at time t_d^{dt} is removed and the quantity removed is $k_{d,t}^{\mathrm{ls}}$ times the original load, there are:

$$\Delta P_{d,t}=u_d(t-t_d^{\mathrm{dt}})k_{d,t}^{\mathrm{ls}}P_{d,t} \tag{10}$$

$$u_d(t-t_d^{\mathrm{dt}})=\begin{cases}1, & t\geqslant t_d^{\mathrm{dt}}\\ 0, & t<t_d^{\mathrm{dt}}\end{cases} \tag{11}$$

$$u_{d,t}=u_d(t-t_d^{\mathrm{dt}}) \tag{12}$$

where $k_{d,t}^{\mathrm{ls}}$ is the reduction factor of the load-shedding device at load node d, which can be determined by the load control strategy; u_d is a state variable with a value of 1 or 0.

After a fault, the equivalent load $P_{d,t}^{\mathrm{eq,f}}$ of node d at any time t is:

$$P_{d,t}^{\mathrm{eq,f}}=P_{d,t}^{\mathrm{f}}-\Delta P_{d,t}^{\mathrm{f}} \tag{13}$$

where $P_{d,t}^{\mathrm{f}}$ is the load at node d after a fault and $\Delta P_{d,t}^{\mathrm{f}}$ is the load power to be cut at node d.

As illustrated in Fig. 7, it is worth noting that power sources and energy storage can be adjusted cooperatively before the loads are switched off at t_d^{cut}.

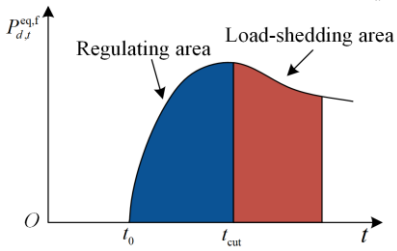

Fig. 7. Providing WDLS by energy storage regulation.

III. Construction of Performance Indexes for WDLS and CELS

To describe the power system's performance in handling WDLS and CELS, a set of indexes are defined in this study, as described below.

A. Node Load Shedding Delay Time, t_d^{dt}

t_d^{dt} is the aforementioned time from the moment of load shedding demand to the time the load is switched off. It represents the duration from the moment node receiving the LSW signal to the execution of the LSC.

B. Maximum Load-shedding Power of Node d, $\Delta P_d^{\max}$

$\Delta P_d^{\max}$ refers to the highest load power that is removed from the designated node d during the load shedding process, i.e.:

$$\Delta P_d^{\max} = \max\{\Delta P_{d,t}\} \tag{14}$$

$\Delta P_{d,t}$, $d \in D$ is the removed load power of the dth load node during the tth period. This implies that the amount of load shed may be alterable.

C. Node Load-shedding Capacity, ΔW_d

This is defined as the cumulative power loss of node d from the initiation of load shedding to the end of the load shedding process, expressed as:

$$\Delta W_d = \sum u_{d,t} \times \Delta P_{d,t} \times \Delta t \tag{15}$$

where Δt is the interval time of the adjustment control command.

D. Node Load-shedding and Recovery Duration, t_d^{dur}

Let t_d^{cut} be the start time of load shedding at node d and t_d^{re} be the time at which the load is recovered, then t_d^{dur} is defined as follows:

$$t_d^{\text{dur}} = t_d^{\text{re}} - t_d^{\text{cut}} \tag{16}$$

When the load is permanently removed, t_d^{re} and t_d^{dur} tend toward infinity.

E. Maximum Delay Time for Load Shedding, $t_d^{\text{dt,max}}$

If the power system requires WDLS at all nodes according to a delay time of the same value, then the maximum value of these delay times $t_d^{\text{dt,max}}$ is defined as the maximum delay time for load shedding, which expresses the adjustment ability of power system energy sources including energy storage. Specifically, in the initial stages following a fault, it is essential to maximize the utilization of the regulation capacity of energy storage and other backup power sources to sustain uninterrupted loads for the longest duration. Beyond this timeframe, a portion or all loads within the network will be shed to maintain system power balance.

IV. Optimization Model of WDLS Based on Energy Storage

As mentioned above, it is necessary to ensure a delay time so that users can prepare for power outages when ELS is inevitable. However, what is the best way of doing this? This section introduces the implementation of WDLS and CELS for comparation.

A. WDLS with Maximum Delay Time for All Load Shedding Nodes (*WDLS/M*)

In a specific system state, considering a power grid with D load nodes, when load reduction becomes inevitable following a fault, one must disconnect a part of the load. When the loads are to be cut off simultaneously, the longest delay time can be selected as a load shedding mode.

As shown in Fig. 8, there are four nodes for load shedding. The disconnected load values are $\Delta P_1 - \Delta P_4$ the delay time is t_1 for all the loads in this mode.

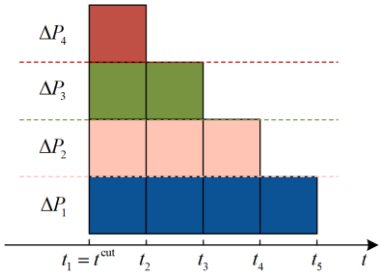

Fig. 8. Simultaneous load shedding.

For multi-node power systems, referring to (7) in Section II, the control constraints after a fault are described below.

1) Power Balance Constraint

$$\sum_{j=1}^{J} P_{j,t}^{\text{f}} + \sum_{e=1}^{E} P_{e,t}^{\text{f}} = \sum_{d=1}^{D} (P_{d,t}^{\text{f}} - \Delta P_{d,t}^{\text{f}}) \tag{17}$$

where $P_{j,t}^{\text{f}}$ is the output of conventional unit j at postfault time t; $P_{e,t}^{\text{f}}$ is the output of energy storage e; $P_{d,t}^{\text{f}}$ is the load at node d; and $\Delta P_{d,t}^{\text{f}}$ is the load power to be cut at node d.

Energy storage power $P_{e,t}^{\text{f}}$ and sheddable load power $\Delta P_{d,t}^{\text{f}}$ are added based on the existing power sources and loads to address network structural changes resulting from faults. Additionally, a control variable $P_j^{\min}$ associated with the load shedding time is set before $\Delta P_{d,t}^{\text{f}}$. It should be noted that changes in energy storage power and capacity will affect the time variable in $P_j^{\min}$, and by adjusting the control variables, the longest delay time $t_d^{\text{dt,max}}$ can be obtained, as:

$$t_d^{\text{dt,max}} = \max\left\{t_d^{\text{dt}}\right\}, \quad d \in D \tag{18}$$

Specifically, load shedding must be controlled according to the follow equation:

$$\Delta P_{d,t}^{\text{f}} = u_d \times (t - t_d^{\text{dt,max}}) \times k_{d,t}^{\text{ls}} P_{d,t}^{\text{f}} \tag{19}$$

where $k_{d,t}^{\text{ls}}$ is the load shedding function of the load shedding device at load node d, determined by the load control strategy.

When $t < t_d^{\text{dt,max}}, u_{d,t} = 0$, and when $t > t_d^{\text{dt,max}}, u_{d,t} \neq 0$.

Following a fault occurrence, once the system's power sources, energy storage, and grid structure are confirmed, the maximum delay time $t_d^{\text{dt,max}}$ can be calculated, alongside the shedding amount at each node, charging and discharging times and power of the energy storage, and generation curves of conventional power sources within the system.

2) Control Constraint of Energy Storage Devices

a) Energy Storage Capacity Constraints

State of charge (SOC) constraints include:

$$B_e^{\mathrm{soc,min}} \leqslant B_{e,t}^{\mathrm{soc,f}} \leqslant B_e^{\mathrm{soc,max}} \tag{20}$$

$$B_{e,t}^{\mathrm{soc,f}} = B_{e,t-1}^{\mathrm{soc,f}} + P_{e,t}^{\mathrm{ch,f}}\Delta t - P_{e,t}^{\mathrm{dis,f}}\Delta t \tag{21}$$

where $B_{e,t}^{\mathrm{soc,f}}$ is the SOC of the energy storage device after the fault; $B_e^{\mathrm{soc,min}}$ and $B_e^{\mathrm{soc,max}}$ are the minimum and maximum limits of the SOC of energy storage device respectively; $P_{e,t}^{\mathrm{dis,f}}$ and $P_{e,t}^{\mathrm{ch,f}}$ are the discharging and charging power of the energy storage device after the fault, respectively.

b) Charge/discharge State Limitation

$$u_{e,t}^{\mathrm{dis,f}} + u_{e,t}^{\mathrm{ch,f}} \leqslant 1 \tag{22}$$

where $u_{e,t}^{\mathrm{dis,f}}$ and $u_{e,t}^{\mathrm{ch,f}}$ are 0–1 variables indicating the discharge and charge states of the energy storage, respectively.

Equation (22) signifies that energy storage can only be in one of the discharging/charging states at each moment.

c) Energy Storage Output Limit

$$0 \leqslant P_{e,t}^{\mathrm{dis,f}} \leqslant P_e^{\mathrm{dis,max}} u_{e,t}^{\mathrm{dis,f}} \tag{23}$$

$$0 \leqslant P_{e,t}^{\mathrm{ch,f}} \leqslant P_e^{\mathrm{ch,max}} u_{e,t}^{\mathrm{ch,f}} \tag{24}$$

where $P_e^{\mathrm{dis,max}}$ and $P_e^{\mathrm{ch,max}}$ are the maximum discharging and charging power of the energy storage device, respectively.

3) Control Constraint on Load Shedding

a) Load Shedding Power Limit

$$0 \leqslant \Delta P_{d,t}^{\mathrm{f}} \leqslant u_{d,t}\Delta P_{d,t}^{\max} u_{d,t}^{\mathrm{q}} \tag{25}$$

where $t_d^{\mathrm{dt}} \neq 0$; $\Delta P_{d,t}^{\max}$ is the maximum power allowed to be disconnected at load node d; and $u_{d,t}^{\mathrm{q}}$ is the state of the load-shedding device, a binary variable taking values of 0 or 1.

b) Load Shedding Capacity Constraint

$$W_d^{\min} \leqslant W_{d,t}^{\mathrm{f}} \leqslant W_d^{\max} \tag{26}$$

$$W_{d,t}^{\mathrm{f}} = W_{d,t-1}^{\mathrm{f}} + \Delta P_{d,t}^{\mathrm{f}}\Delta t \tag{27}$$

where $W_{d,t}^{\mathrm{f}}$ represents the capacity of the load shedding of node d during the duration of load shedding; $W_d^{\min}$ and $W_d^{\max}$ denote the minimum and maximum loads.

c) Load Shedding Control Limitation

$$u_{d,t}^{\mathrm{q}} + u_{d,t}^{\mathrm{bq}} \leqslant 1 \tag{28}$$

where $u_{d,t}^{\mathrm{q}}$ and $u_{d,t}^{\mathrm{bq}}$ are binary variables (0 or 1) representing whether the load is to be decreased or not.

4) Control Constraint on Power Sources

a) Generator Output and Start/Stop Constraints

Unit output constraints are specified as:

$$P_j^{\min} \leqslant P_{j,t}^{\mathrm{f}} \leqslant P_j^{\max} \tag{29}$$

where $P_j^{\max}$ and $P_j^{\min}$ denote the maximum and minimum output limits for unit j, respectively.

b) Spare Capacity Limit

$$u_{j,t}^{\mathrm{f}} P_{j,t}^{\mathrm{f}} \leqslant (1-\alpha) P_j^{\max} \tag{30}$$

where $u_{j,t}^{\mathrm{f}}$ represents the start or stop state of unit j after the fault; and α is the unusable factor.

c) Unit Climbing Limit

$$P_{j,t}^{\mathrm{f}} - P_{j,t-1}^{\mathrm{f}} \leqslant R_{j,\mathrm{u}} \tag{31}$$

$$P_{j,t-1}^{\mathrm{f}} - P_{j,t}^{\mathrm{f}} \leqslant R_{j,d} \tag{32}$$

where $R_{j,\mathrm{u}}$ denotes the upward climbing rate of unit j; and $R_{j,d}$ is the downward climbing rate. For upward climbing, the power at time t must be greater than that at time $t-1$, ensuring that $P_{j,t}^{\mathrm{f}} - P_{j,t-1}^{\mathrm{f}} > 0$. The downward climbing constraint is similar.

d) Unit Start/Stop Time Limit

$$\sum_{k=t}^{t+T_j^{\mathrm{U}}-1} u_{j,k}\Delta t \geqslant T_j^{\mathrm{U}} \times \left(u_{j,t} - u_{j,t-1}\right) \tag{33}$$

$$\sum_{k=t}^{t+T_j^{\mathrm{D}}-1} u_{j,k}\Delta t \leqslant T_j^{\mathrm{D}} \times \left(1 + u_{j,t} - u_{j,t-1}\right) \tag{34}$$

where k is the start/stop time of the unit; while T_j^{U} and T_j^{D} are the minimum start/stop times of the generating unit, whose values are set according to the unit's intrinsic start/stop time; $u_{j,k}$ is the state of generator control, where "1" means the unit is permitted and "0" means not permitted.

5) Network Transmission Constraint

a) Element Power Flow Constraint

$$0 \leqslant P_{\mathrm{l},t}^{\mathrm{f}} \leqslant P_{\mathrm{l}}^{\max} \tag{35}$$

where $P_{l,t}^{\mathrm{f}}$ is the power transmitted by branch l at time t after the fault; and $P_{\mathrm{l}}^{\max}$ represents the maximum limit of transmitted power, constrained by the state stability.

b) Line Thermal Stability Constraint

$$T_{\mathrm{ol}}^{\mathrm{f}} < T_{\mathrm{ol}}^{\max} \tag{36}$$

where $T_{\mathrm{ol}}^{\mathrm{f}}$ represents the transmission line temperature; and $T_{\mathrm{ol}}^{\max}$ is the maximum allowed temperature to maintain the thermal stability of the line.

B. WDLS with Different Delay Time for Different Load Shedding Nodes (*WDLS/D*)

In real systems, owing to variations in load characteristics and differences in the status of users' backup power sources, the required outage preparation time varies among users. There are different loss characteristics for different users when load shedding occurs. Therefore, the load shedding delay time may also differ. This approach should be supported by different load shedding delay times and regulatory resources, including

energy storage. The schematic of load shedding and representation is illustrated in Fig. 9.

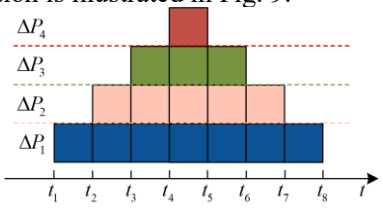

Fig. 9. Load shedding with different delay times.

In Fig. 9, loads $\Delta P_1 - \Delta P_4$ are sequentially disconnected from various nodes, with a delay time from t_1 to t_4.

Assuming that there are different tolerance times, t_d^{set}, in user nodes; and $u_{d,t}^{\text{dt,set}}$ is the state of the load-shedding device, a binary variable taking values of 0 or 1. The load shedding delay time can be defined as:

$$t_d^{\text{dt}} = t_d^{\text{set}}, \quad d \text{ is from 1 to } D \tag{37}$$

$$u_{d,t} = u_{d,t}^{\text{dt,set}}, \quad d \text{ is from 1 to } D \tag{38}$$

The objective function aims to minimize the sum of the load cutting power in each period, i.e.:

$$\min \Delta W = \sum_{t=1}^{T} \sum_{d=1}^{D} \Delta W_{d,t}^{\text{f}} \tag{39}$$

where ΔW is the total amount of power capacity removed from the start of load cutting to load restoration; and $\Delta W_{d,t}^{\text{f}}$ is the amount of load cut at the dth load node at time t, given as:

$$\Delta W_{d,t}^{\text{f}} = (P_{d,t}^{\text{f}} - P_{d,t-1}^{\text{f}}) \times \Delta t \tag{40}$$

where $P_{d,t}^{\text{f}}$ and $P_{d,t-1}^{\text{f}}$ are the loads of node d at time t and $t-1$, respectively.

The power balance control equations and constraints are consistent with those described earlier. By solving the aforementioned objective function with the constraints, we can obtain the curves of power generation units, storage energies to be discharged or charged, and load power to be cut at the corresponding delay time for each load.

C. Conventional Emergency Load Shedding without Delay Time

Currently, in power systems requiring emergency load shedding, the typical approach involves the application of the minimum load shedding control method [6], without implementing WDLS strategies.

The control model for load shedding can be adjusted as:

$$\Delta P_{d,t}^{\text{f}} = u_d (t - t_d^{\text{dt}}) k_{d,t}^{\text{ls}} P_{d,t}^{\text{f}} \tag{41}$$

where $t_d^{\text{dt}} = 0$, and load shedding is promptly executed based on the requirement that the system power should balance the network constraints.

Typically, the minimum load shedding objective is adopted, as indicated in (39), with constraints including power generation regulation and network transmission. Thus, the control curves for each control variable can be calculated.

Through calculations, a comparison between the two load shedding models can be made, providing evidence for selecting different models.

V. Simulations of Multi-mode Emergency Load-shedding Control

To validate the aforementioned load-shedding strategy, the IEEE 30-node system is used as an example, shown in Fig. 10. In this system, $G_1 - G_5$ represent thermal power units. The power supply is concentrated in upper area 1 of the network, whereas the loads are concentrated in lower area 2. Power is transmitted through several link lines, namely, $L_{4-12}, L_{6-9}, L_{6-10}, L_{9-10}$, and L_{28-27}.

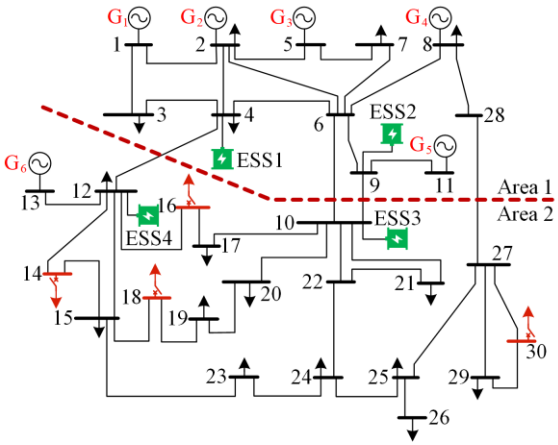

Fig. 10. IEEE 30-node power system diagram.

In power receiving area 2, the power source, G_6, is a hydroelectric power station, which serves as a backup power source for the load. Energy storages are configured at node 4 and node 9 in power sending area 1, and at node 16 and node 10 in receiving area 2.

This study aims to illustrate the principle of WDLS in the severe fault scenario. Assuming the following fault scenario: two transmission lines (L_{6-10}, L_{6-8}) in the network are tripped consecutively by protection relays, resulting in overloading of some remaining lines, such as L_{4-12}, L_{9-10}. To limit the current on overloaded lines within a safe range, load-shedding control must be implemented.

The fault trip time is set to the 5th minute, and the initial power storage capacity of each node is 50%. The load shedding devices are activated at nodes 14, 16, 18, and 30. The simulation results of the output power of generation units as well as states of energy storages and load shedding devices can be observed by linearizing the optimal modes and solving the equations with the CPLEX tool.

A. Simulation and Indexes of WDLS/M

In Table I, t_d^{dt} represents the maximum load shedding delay time of each node; $\Delta P_d^{\max}$ corresponds to the total node's maximum load shedding power; ΔW_d indicates the node's load-shedding capacity; and t_d^{dur} displays the node's load shedding and recovery duration.

TABLE I
INDEXES OF WDLS/M STRATEGY

	Node	14	16	18	30
ESS is 100%	t_d^{dt} (min)	13	13	13	13
	$\Delta P_d^{\max}$ (MW)	31	26	23	26
	ΔW_d (MWh)	14.25	14.25	14.25	14.25
	t_d^{dur} (min)	45	48	51	48
ESS is 50%	t_d^{dt} (min)	7	7	7	7
	$\Delta P_d^{\max}$ (MW)	32	37	53	37
	ΔW_d (MWh)	14.78	14.89	15.08	14.89
	t_d^{dur} (min)	59	58	45	58

The results show that when the amount of energy storage is 100%, the maximum load-shedding delay time at each node is 13 min. Whereas the power and duration of load shedding vary at each node, the allocated load shedding power capacity is held constant. The total load power, $P_{d,t}^{\mathrm{eq,f}}$ is depicted in Fig. 11.

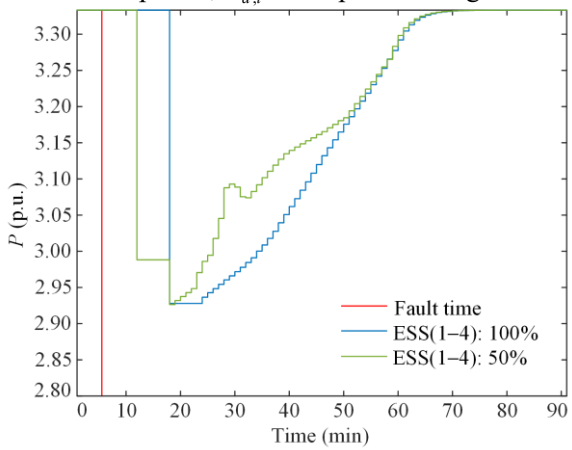

Fig. 11. Total load power $P_{d,t}^{\mathrm{eq,f}}$ curve in WDLS/M.

After fault occurs at the 5th minute, there is a delay time until the 18th minute to initiate load shedding, which persists for a certain period, followed by gradual recovery. At the 68th minute, the cutoff power reaches 0, indicating full load recovery.

It can be seen from Table I and Fig. 11 that, when the power and capacity of energy storage decrease, the maximum delay in load shedding reduces (7 min for 50% ESS). Moreover, the peak power of load shedding at each node increases, along with the duration of the load shedding process. This reflects the significant impact of energy storage on the system's capacity for delaying load shedding.

Figure 12 shows the generator output curves. Following fault occurrence (at the 5th minute), a shift is observed in the system current distribution. To prevent temperature overruns on lines L_{4-12} and L_{9-10} to maximize the load-shedding delay, adjustments are made to the generator control:

Unit G_1, located farthest from the load center area, undergoes a significant downward adjustment of output power because the transmission is crowded. Similarly, the output power of units G_3, G_5 also decrease. Close to the link line area, units G_2, G_4 adjust their output powers upward. The standby unit at the receiving area, G_6, continues to adjust its output power upward. This adjustment strategy is implemented to optimize the load-shedding delay and prevent temperature overruns on critical transmission lines.

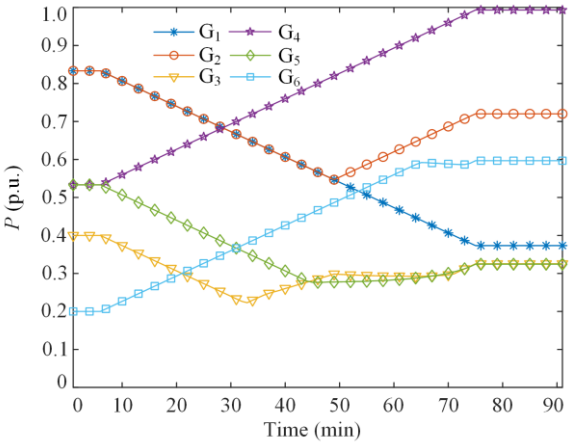

Fig. 12. Output power of generators in WDLS/M.

To postpone load shedding, following the fault at the 5th minute, ESS3 and ESS4 at the receiving area initiate discharging, and meanwhile, ESS1 and ESS2 are charged and discharged alternately to alleviate the overload of link lines and balance the power without load shedding. The results are shown in Fig. 13.

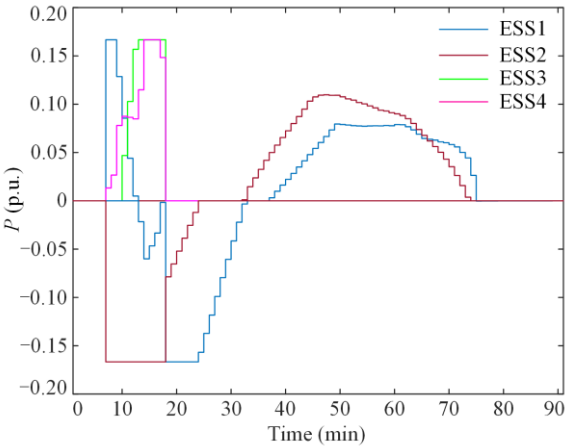

Fig. 13. Output power of energy storages in WDLS/M (ESS: 100%).

Figure 14 displays the load shedding sharing curves, which indicated that the load cutting time of the four users are the same at the 18th minute, i.e., the load-shedding delay time is 13 min. However, the power of load shedding at each node vary, depending on the load size and location.

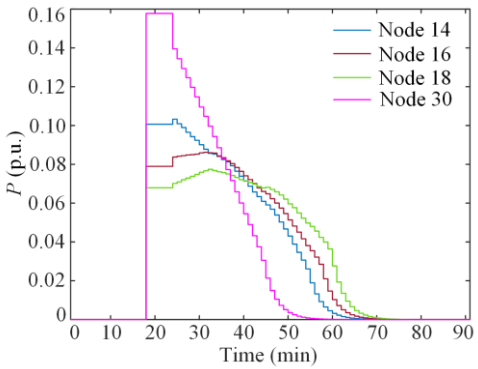

Fig. 14. Time of load shedding and load power values in WDLS/M (ESS: 100%).

The power curves and temperatures of link lines between the sending and receiving areas are depicted in Fig. 15. It shows that the power flows on L_{4-12}, L_{9-10} violently increase initially after the fault occurrence, and then decrease rapidly when the control action begins. The temperatures on these lines are controlled below the permitted value of 70 ℃.

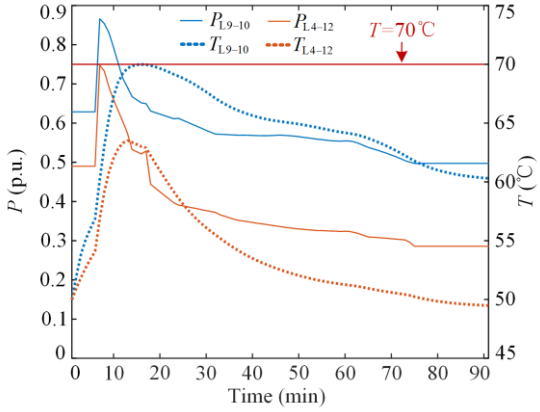

Fig. 15. Power flow and temperature of link lines in WDLS/M (ESS: 100%).

B. Simulation and Indexes of WDLS/D

Assuming that, based on load characteristics, nodes 14, 16, 18, and 30 are designed to have different tolerable delay times for load-cutting delays of 5, 10, 15, and 10 min, respectively, in the aforementioned scenario. Then, the WDLS/D load shedding mode can be used for minimum power loss, and the simulation results for this scenario are presented in Table II.

TABLE II
INDEXES OF WDLS/D STRATEGY

	Node	14	16	18	30
ESS is 100%	t_d^{dt} (min)	5	∞	15	10
	ΔP_d^{max} (MW)	22	0	42	56
	ΔW_d (MWh)	2.78	0	12.15	14.25
	t_d^{dur} (min)	10	0	27	28
ESS is 50%	t_d^{dt} (min)	5	5	15	10
	ΔP_d^{max} (MW)	18	60	57	60
	ΔW_d (MWh)	2.59	11.45	15	15.25
	t_d^{dur} (min)	10	13	29	25

The optimization results reveal that, when the amount of energy storage is 100%, the load at the 16th node remains unaffected, whereas the other three nodes undergo load cutting in accordance with the predetermined delay time. Node 30 carries out load resection with the highest power, greatest amount of power capacity resected, and longest duration of load shedding. This is because node 30 bore the heaviest load.

When energy storage decreases by 50%, the peak power of load shedding at each node increases, resulting in an increase in the amount of load shed.

The total load profile, considering load cutting, is shown in Fig. 16. As seen, it is evident that the load-shedding operation is executed during specific time intervals with predetermined delays.

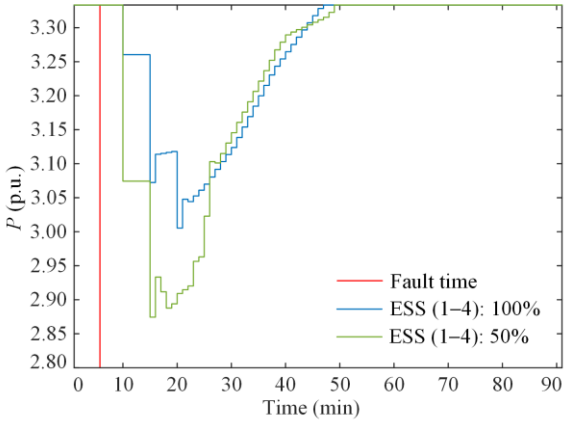

Fig. 16. Total load power $P_{d,t}^{eq,f}$ curve in WDLS/D.

Observing the generator output curve in Fig. 17, it is apparent that the generating units have successfully completed regulation, reaching the new steady state at the 75th minute. This strategy has a similar effect on WDLS/D when starting emergency control.

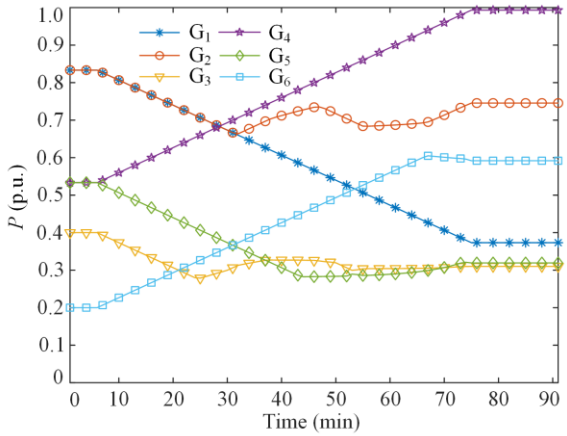

Fig. 17. Output power of generators in WDLS/D (ESS: 100%).

From the output power of the energy storages shown in Fig. 18, it can be seen that ESS3 and ESS4 in the receiving area are discharged rapidly to compensate for the user's load demand after failure. Simultaneously, the storage at the sending area is discharged or charged depending on the need to satisfy the transmission constraints.

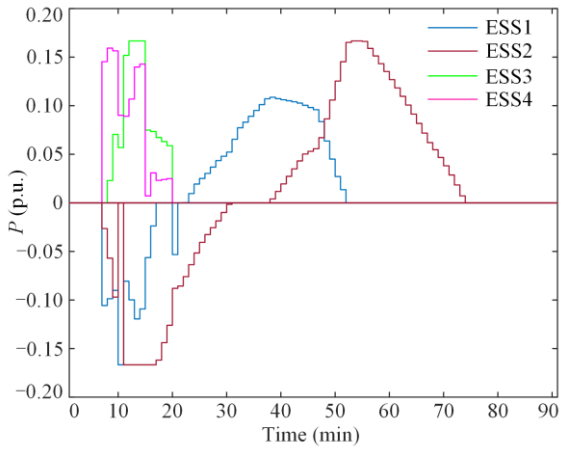

Fig. 18. Output power of energy storages in WDLS/D (ESS: 100%）.

Figure 19 shows the load shedding sharing curves, while Fig. 20 shows that the power flow and temperature of the link lines. As seen from Fig. 20, temperatures of L_{4-12}, L_{9-10} can also be controlled within the permitted values.

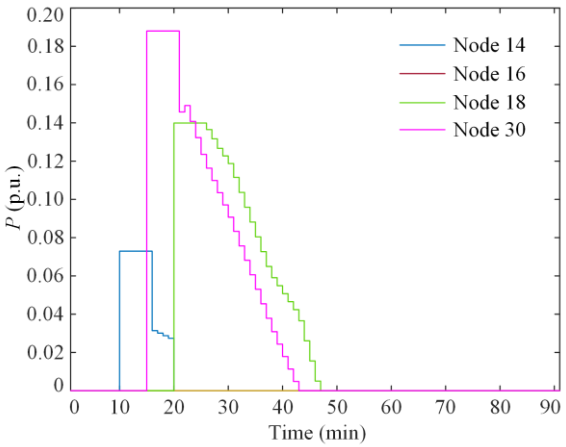

Fig. 19. Time of load shedding and load power values in WDLS/D (ESS: 100%).

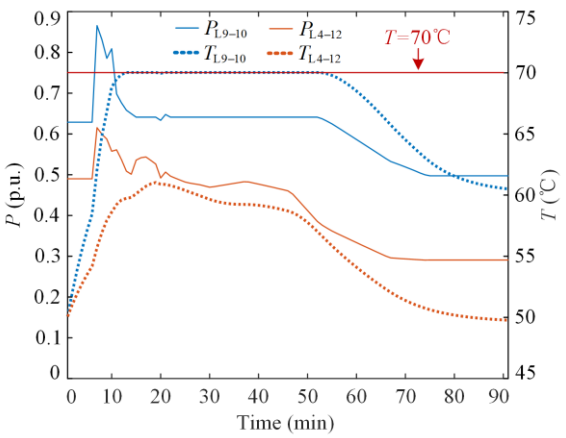

Fig. 20. Power flow and temperature of link lines in WDLS/D (ESS: 100%).

C. Simulation and Indexes of CELS

With the objective of minimizing the amount of load cutting, load cutting is executed based on the network's inherent security constraints without accounting for the load shedding delay. The computed results are presented in Table III.

TABLE III
INDEXES OF CELS STRATEGY

	Node	14	16	18	30
ESS is 100%	t_d^{dt} (min)	∞	∞	7	1
	ΔP_d^{max} (MW)	0	0	31	46
	ΔW_d (MWh)	0	0	14.25	14.25
	t_d^{dur} (min)	0	0	34	32
ESS is 50%	t_d^{dt} (min)	∞	6	7	1
	ΔP_d^{max} (MW)	0	20	36	49
	ΔW_d (MWh)	0	28	14.85	15.07
	t_d^{dur} (min)	0	25	34	27

It is evident that when the amount of energy storage is 100%, and in the absence of the delayed load-cutting strategy, nodes 14 and 16 are excluded from the load shedding scheduling. Instead, load shedding is centrally coordinated at nodes 18 and 30, which exhibits a higher load shedding capacity. Node 30 undergoes load shedding 1 min after the fault, whereas node 18 experiences load shedding after a 7 min delay. When the energy storage is decreased by 50%, the load shedding power is evidently increased.

By analyzing the total load curve shown in Fig. 21, it becomes apparent that the load shedding device initiates action 1 min after the fault. Without considering any delay, the load-shedding magnitude can be reduced by immediately activating the load-shedding mechanism at the time of the fault.

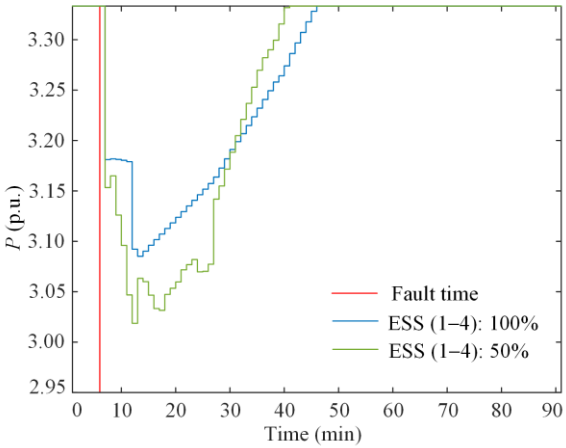

Fig. 21. Total load power $P_{d,t}^{eq,f}$ curve in CELS.

Observing the generator output curve in Fig. 22, it is apparent that the generating units have successfully completed regulation, also reaching the new steady state at the 75th minute.

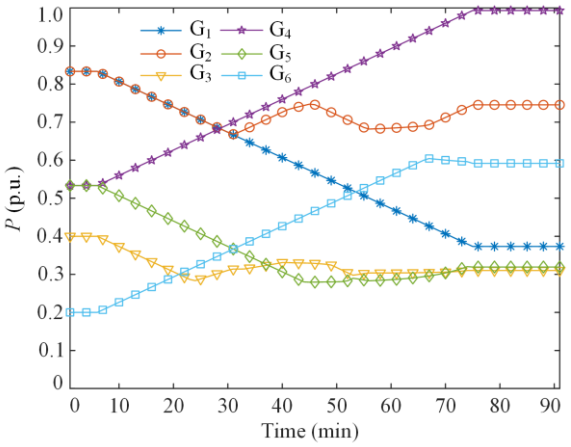

Fig. 22. Output power of generators in CELS (ESS: 100%).

Examining the storage discharge curve in Fig. 23 reveals that storage unit ESS4 at the receiving end undergoes rapid discharge following the fault, with subsequent involvement of other storage units in the regulation process.

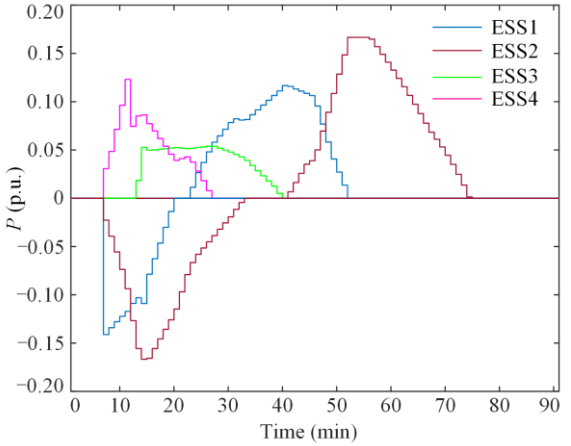

Fig. 23. Output power of energy storages in CELS (ESS: 100%).

Figure 24 shows the load shedding sharing curves, while Fig. 25 shows that the power flow and temperature of the link lines, indicating the temperatures of the links are also controlled within the permitted values.

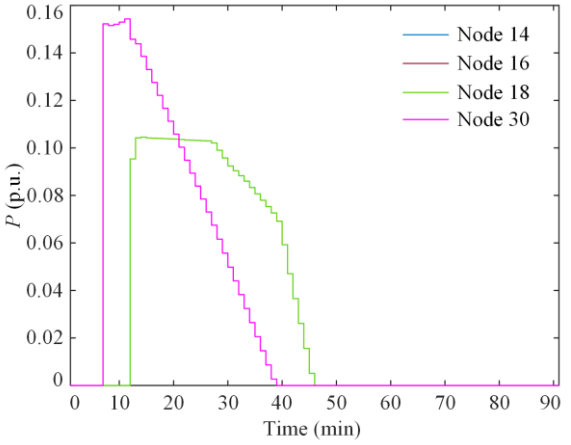

Fig. 24. Time of load shedding and load power values in CELS (ESS: 100%).

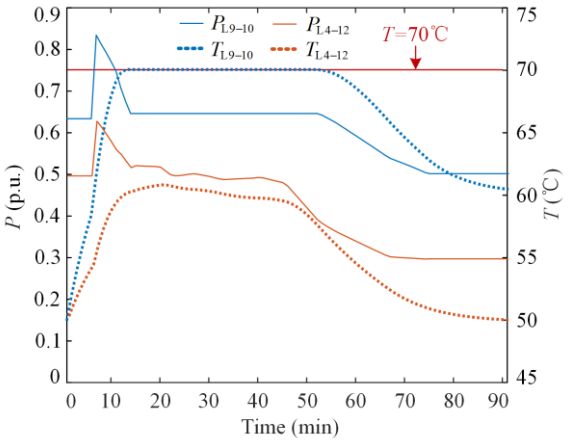

Fig. 25. Power flow and temperature of link lines in CELS (ESS: 100%).

D. Comparison of Load Shedding Models

A comparative analysis of the indices of the aforementioned three load shedding strategies is presented in Table IV.

TABLE IV
INDEXES OF CELS STRATEGY

	Method	WDLS/M	WDLS/D	CELS
ESS is 100%	Duration (min)	51	28	34
	Min delay time (min)	13	5	1
	Max delay time (min)	13	15	7
	Max node power (MW)	47	56	46
	Total energy (MWh)	57	29.18	28.5
ESS is 50%	Duration (min)	59	29	34
	Min delay time (min)	7	5	1
	Max delay time (min)	7	15	7
	Max node power (MW)	57	60	49
	Total energy (MWh)	59.83	44.29	34.2

It can be observed that the WDLS/M strategy has the longest delay time, load shedding duration, and maximum load shedding power. In contrast, the WDLS/D strategy focuses on removing loads based on specified delay times, resulting in a slightly greater amount of shed power but with the shortest duration of load shedding. The CELS strategy, however, swiftly removes portions of the load without considering load shedding delay, leading to the smallest total amount of shed power.

The findings indicate that, to obtain the maximum load shedding delay time, such as in the WDLS/M strategy, greater power loss or a longer recovery time may be required. In reality, delays of a few minutes may be enough for many users to prepare for electricity outages, as in the case of the WDLS/D strategy, while having small increase in the power and quantity of shed load power when compared to the results obtained in the CELS strategy without a load shedding delay.

VI. Conclusion

It is known that electricity users suffer from the stress of sudden electricity outages due to the need for emergency control of the power network. Considerable efforts have been made to decrease the impact of power source interruption. From the knowledge of disaster prevention, if users have time to prepare before electricity interruption, their losses can be minimized. To ensure a warning and delay time for users when emergency control requires load shedding, this study proposes an innovative method for utilizing the energy storage and backup power of other generators in a power system. The key findings of this study are summarized below.

1) Enhancing in-phase regulation and control capabilities, issuing power outage warnings, and bolstering the emergency response capabilities of users are imperative for alleviating the social and economic impacts of emergency load cuts during grid failures.

2) By incorporating energy storage and time-varying switch functions into the traditional power balance equation, flexible control over energy storage regulation and load shedding moments can be achieved. Furthermore, implementing the maximum delay time for load shedding is also viable.

3) It is also feasible to apply different load shedding delay times for users with different delay requirements, thus enhancing the flexibility of emergency load shedding, while ensuring minimum load shedding.

4) Several indicators (load shedding delay time, load shedding maximum power, load shedding power, and load shedding duration) are introduced to accurately reflect the abilities of emergency load shedding regulations.

Acknowledgment

Not applicable.

Authors' Contributions

Pengfei Yu: conceptualization, methodology, software, case study, investigation, formal analysis, writing-original draft, and writing-review & editing. Xiaofu Xiong: conceptualization, project administration, and supervision. Xiangzhen He: software and case study. Jizhong Zhu: data curation, resources, supervision, and validation. Jun Liang and Dongliang Nan: supervision. All authors read and approved the final manuscript.

Funding

This work is supported by the National Natural Science Foundation of China (No. 52077017).

Availability of Data and Materials

Not applicable.

Declarations

Competing interests: The authors declare that they have no known competing financial interests or personal relationships that could have appeared to influence the work reported in this article.

Authors' Information

Pengfei Yu obtained his Ph.D. in electrical engineering from the School of Electrical Engineering, Chongqing University in 2024. He is currently working at Chongqing Hui Zhi Energy Co., Ltd., Chongqing, China. He used to exchange academics for two years with the School of Engineering at Cardiff University in 2019 and 2021. His research interests include power system operation and control, clean energy, energy storage and analysis of new power system.

Xiaofu Xiong is a professor, doctoral supervisor, IEEE/IET/CSEE Fellow, in Chongqing University. Main research interests: power system protection and control, smart grid and smart substation technology, new energy grid-connected fault analysis, power grid risk assessment and meteorological disaster warning, energy storage applications, etc.

Xiangzhen He is currently working toward the M.S. degree in electrical engineering with the School of Electrical Engineering, Chongqing University, Chongqing, China. His research interests include power system protection and control and analysis of new power system.

Jizhong Zhu is a professor and doctoral supervisor. He is a member of the European Academy of Sciences and Arts, a foreign member of the Italian Bologna Academy of Sciences, an IEEE/ET/CSEE/AIIA Fellow, and the team leader of AISI at South China University of Technology. His main research interests include optimized operation and control of integrated intelligent energy systems.

Jun Liang is currently a professor in the School of Engineering at Cardiff University, UK. He has long been engaged in research on power systems and energy technologies, with key focuses including high-voltage direct current transmission (HVDC), DC grids, power electronics and converter control, wind power generation, and grid integration.

Dongliang Nan is a senior engineer, deputy director of Grid Technology Research Institute, State Grid Xinjiang Electric Power Research Institute.

References

[1] A. Lei, J. Zhou, and Y. Mei *et al*., "Analysis and lessons of the blackout in Chinese Taiwan power grid on March 3, 2022," *Southern Power System Technology*, vol. 16, no. 9, pp. 90-972, May 2022. (in Chinese)

[2] H. Zhong, G. Zhang, and T. Cheng *et al.*, "Analysis and enlightenment of extremely cold weather power outage in Texas, U.S. in 2021," *Automation of Electric Power Systems*, vol. 46, no. 6, pp. 1-9, Mar. 2022. (in Chinese)

[3] C. Fan, J. Yao, and Q. Zhuang *et al*., "Reflection and analysis for oscillation of the blackout event of 9 August 2019 in UK," *Electric Power Engineering Technology*,

vol. 39, no. 4, pp. 34-41, Jul. 2020. (in Chinese)
[4] L. Li, L. Ji, and Y. Zhang *et al*., "Preliminary analysis and Lessons of Blackout in Pakistan Power Grid on January 9, 2021," *Power System Technology*, vol. 46, no. 2, pp. 655-663, May 2022. (in Chinese)
[5] L. Xu, K. Feng, and N. Lin *et al.*, "Resilience of renewable power systems under climate risks," *Nature Reviews Electrical Engineering*,vol. 1, pp. 53-66. Jan. 2024.
[6] Z. Wang, S. Zhu, and T. Wang *et al*., "Research on stratified optimal load shedding strategy for receiving end power grid," *Transactions of China Electrotechnical Society*, vol. 35, no. 5, pp. 1128-1139, Dec. 2020. (in Chinese)
[7] Y. Wen, C. Y. Chung and X. Ye. "Enhancing frequency stability of asynchronous grids interconnected with HVDC links," *IEEE Transactions on Power Systems*, vol. 33, no. 2, pp. 1800-1810, Mar. 2018.
[8] Z. Hu, L. Zeng, and W. Yao *et al*., "Intelligent pre-decision of two-stage emergency load shedding control in power systems," *Proceedings of the CSEE*, vol. 44, no. 4, pp. 1-13, Feb. 2024 (in Chinese)
[9] M. Liu, T. Xu, and C. Li *et al*., "Optimization of emergency load shedding of receiving-end power grid based on particle swarm optimization," *Journal of Shandong University (Engineering Edition)*, vol. 49, no. 1, pp. 120-128, Feb. 2019. (in Chinese)
[10] C. Qin, W. Ren, and Y. Jiang *et al*., "Coordinated optimization strategy of wheel load shedding under frequency safety subsection control," *Electric Power Automation Equipment*, vol. 42, no. 7, pp. 261-268, May 2022. (in Chinese)
[11] S. Liao, Y. Chen, and J. Xu *et al*., "Emergency load shedding control method for renewable power system based on feeder load disaggregation," *Power System Technology*, vol. 47, no. 11, pp. 4405-4417, Jan. 2023. (in Chinese)
[12] John Romano, "Distributed system implementation plan," Consolidated Edison Inc, New York State Electric & Gas and Rochester Gas and Electric, New York, USA, 2023.
[13] X. Dong, K. Xu, and H. Zou *et al*., "Research on emergency power supply strategy for important users of distribution network under large area blackout," *Journal of Safety Science and Technology*, vol. 19, no. 3, pp. 33-38, Mar. 2023. (in Chinese)
[14] A. Cattaneo, S. C. Madathil, and S. Backhaus. "Integration of optimal operational dispatch and controller determined dynamics for microgrid survivability," *Applied Energy*, vol. 230, pp. 1685-1696, Nov. 2018.
[15] W. Du, R. H. Lasseter, and A. S. Khalsa. "Survivability of autonomous microgrid during overload events," *Transactions on Smart Grid*, vol. 10, no. 4, pp. 3515-3524, Jul. 2019.
[16] C. Sheetal, A. B. Pritam, and P. K. Rout. "Load shedding strategy coordinated with storage device and D-STATCOM to enhance the microgrid stability," *Protection and Control of Modern Power Systems*, vol. 4, no. 3, pp. 1-19, Jul. 2019.
[17] M. M. Elwakil, H. M. El Zoghaby, and S. M. Sharaf *et al.*, "Adaptive virtual synchronous generator control using optimized bang-bang for islanded microgrid stability improvement," *Protection and Control of Modern Power Systems*, vol. 8, no. 4, pp. 1-21, Oct. 2023.
[18] N. Kadel, W. Sun, and Q. Zhou, "On battery storage system for load pickup in power system restoration," in *2014 IEEE PES General Meeting|Conference & Exposition*, National Harbor, USA, Jul. 2014, pp. 1-5.
[19] X. Dong, K. Xu, and H. Zou *et al.*, "Research on emergency power supply strategy for important users of distribution network under large area blackout," *Journal of Safety Science and Technology*, vol 19, no. 3, pp. 33-38, Mar. 2023. (in Chinese)
[20] W. Lauwers, A. McGuire, and P. Holloway *et al*., "Mobile energy storage study: emergency response and demand reduction," Massachusetts Department of Energy Resources, Boston, USA, 2020.
[21] Y. Sun, J. Zhong, and Z. Li *et al.*, "Stochastic scheduling of battery-based energy storage transportation system with the penetration of wind power," *IEEE Transactions on Sustainable Energy*, vol. 8, no. 1, pp. 135-144, Jan. 2017.
[22] H. H. Abdeltawab and Y. A. R. I. Mohamed, "Mobile energy storage scheduling and operation in active distribution systems," *IEEE Transactions on Industrial Electronics*, vol. 64, no. 9, pp. 6828-6840, Sep. 2017.
[23] Y. Wang, K. Tan, and X. Peng *et al.*, "Coordinated control of distributed energy-storage systems for voltage regulation in distribution networks," *IEEE Transactions on Power Delivery*, vol. 31, no. 3, pp. 1132-1141, Jun. 2016.
[24] D. Zhang, J. Li, and D. Hui, "Coordinated control for voltage regulation of distribution network voltage regulation by distributed energy storage systems," *Protection and Control of Modern Power Systems*, vol. 3, no. 1, pp. 1-8, Jan. 2018.
[25] X. Li, R. Ma, and W. Gan *et al*., "Optimal dispatch for battery energy storage station in distribution network considering voltage distribution improvement and peak load shifting," *Journal of Modern Power Systems and Clean Energy*, vol. 10, no. 1, pp. 9-19, Jan. 2022.
[26] W. Hu, T. Zheng, and P. Du, *et al.*, "An intelligent assisted assessment method for distribution grid engineering quality based on large language modelling and ensemble learning," *Protection and Control of Modern Power Systems*, vol. 10, no. 3, pp. 83-97, May 2025.
[27] Specific configuration of power supply and self-emergency power supply for important power users, GB/T 29328-2018, 2018. (in Chinese)
[28] J. Tang and J. Huang, "Analysis of time characteristics of standby power supply and electric source for safety services," *Building Electricity*, vol. 42, no. 11, pp. 36-40, Nov. 2023. (in Chinese)
[29] Y. Yin. "COPA: highly cost-effective power back-up for green data centers," *IEEE Transactions on Parallel and Distributed Systems*, vol. 31, no. 4, pp. 967-980, Oct. 2020.
[30] S. Su, K. Li, and W. Chan *et a1*., "Agent-based self-healing protection system," *IEEE Transactions on Power Delivery*, vol. 21, no. 2, pp. 610-618, Apr. 2006.
[31] Y. Lin, H. Luo, and Y. Chen *et al*., "Enhancing participation of widespread distributed energy storage systems in frequency regulation through partitioning-based control," *Protection and Control of Modern Power Systems*, vol. 10, no. 1, pp. 76-89, Jan. 2025.
[32] NFPA 99: Standard for health care facilities, 1996.
[33] NFPA 110: Standard for Emergency and Standby Power Systems, 2005.
[34] IEEE draft recommended practices and requirements for harmonic control in electric power systems, IEEE Std 519-2014 (Revision of IEEE Std 519-1992), 2013.
[35] Z. Yang, H. Wang, and Z. Yan *et al.*, "Research and development of device of millisecond precise load control system," *Process Automation Instrumentation*, vol. 39, no. 11, pp. 11-16, Nov. 2018. (in Chinese)